LETTERS

Advancing decadal-scale climate prediction in the North Atlantic sector

N. S. Keenlyside[1], M. Latif[1], J. Jungclaus[2], L. Kornblueh[2] & E. Roeckner[2]

The climate of the North Atlantic region exhibits fluctuations on decadal timescales that have large societal consequences. Prominent examples include hurricane activity in the Atlantic[1], and surface-temperature and rainfall variations over North America[2], Europe[3] and northern Africa[4]. Although these multidecadal variations are potentially predictable if the current state of the ocean is known[5–7], the lack of subsurface ocean observations[8] that constrain this state has been a limiting factor for realizing the full skill potential of such predictions[9]. Here we apply a simple approach—that uses only sea surface temperature (SST) observations—to partly overcome this difficulty and perform retrospective decadal predictions with a climate model. Skill is improved significantly relative to predictions made with incomplete knowledge of the ocean state[10], particularly in the North Atlantic and tropical Pacific oceans. Thus these results point towards the possibility of routine decadal climate predictions. Using this method, and by considering both internal natural climate variations and projected future anthropogenic forcing, we make the following forecast: over the next decade, the current Atlantic meridional overturning circulation will weaken to its long-term mean; moreover, North Atlantic SST and European and North American surface temperatures will cool slightly, whereas tropical Pacific SST will remain almost unchanged. Our results suggest that global surface temperature may not increase over the next decade, as natural climate variations in the North Atlantic and tropical Pacific temporarily offset the projected anthropogenic warming.

The North Atlantic is a region with large natural multidecadal variability[2,4,11–14]. Observations suggest that Atlantic multidecadal variability may be oscillatory, with a period of 70–80 years. Palaeo-evidence[15] and coupled general circulation models[16–18] support the oscillatory nature of Atlantic multidecadal variability, and hence the existence of a low order mode of natural variability. Although major uncertainties exist in the mechanisms of Atlantic multidecadal variability[19], it is widely accepted that the meridional overturning circulation (MOC) plays an important role in driving multidecadal SST variations, as shown by ocean[20] and coupled[5,7,14,16,19] model simulations.

Studies with coupled general circulation models assuming perfect ocean initial conditions indicate that accurate initialization of MOC may allow Atlantic multidecadal variability to be predicted a decade or more in advance[5–7]. However, past MOC fluctuations have been poorly observed[8] and large uncertainties exist among ocean model simulations[21] and ocean analyses. Here, this difficulty is partly overcome with a simple initialization scheme, previously applied in seasonal forecasting[22], that consists of relaxing SST anomalies of the coupled general circulation models to observations. (These simulations, called SST-restored, are described in Methods.) Additionally, decadal predictions require accurate projections of external radiative

forcing (that is, computed from concentrations of greenhouse gases and sulphate aerosols, solar cycle variations, and volcanic activity)[10,23].

Using this simple initialization technique and a state-of-the-art coupled general circulation model[24], a set of ten-year-long, three-member ensemble hindcasts/forecasts were performed every five years from 1955 till 2005 (except for 1995, which instead is started in 1994). External radiative forcing in the hindcasts is treated following ref. 9. Three additional integrations with radiative forcing computed following observations (called twentieth century-RF) are used to estimate predictability due to external radiative forcing. (See Methods for experimental details.)

Skilful predictions of surface temperature averaged over years one to ten of the hindcasts are obtained over large parts of the North Atlantic, Europe, North America and northern Africa (Fig. 1a). In these regions, skill is well above that of persistence (Fig. 1b). Persistence, the prediction that assumes no change from the initial conditions, is a commonly used benchmark for skill. The twentieth century-RF simulations show skill over parts of northern Africa, North America and Europe, but no skill over the North Atlantic Ocean, except in the vicinity of the Equator (Fig. 1c). Over the northern North Atlantic, the climate model hindcast is significantly more skilful than the twentieth century-RF simulations (Fig. 1a). It follows that in this region a significant fraction of the skill arises from initialization of the North Atlantic Ocean, as opposed to external radiative forcing. Over western Europe and large parts of North America, initialization also leads to a significant enhancement in skill. Skill enhancements outside the North Atlantic sector are found in the central eastern tropical Pacific (Fig. 1a and below) and the equatorial Indian Ocean (Supplementary Information).

In several regions, initialization causes a significant degradation in skill compared to the twentieth century-RF simulations (Fig. 1c). Over the tropical North Atlantic and central Africa this is probably related to deficiencies, common to many coupled models, in simulating tropical Atlantic climate. Thus, large skill improvements in this region may be expected, as models improve. The SST-restored simulations (Fig. 1d) provide an estimate for the upper limit of skill of our forecast system during the period considered, as they include observed SST anomalies and external radiative forcing. Over all three land regions, the skill of the SST-restored simulations is generally higher and larger in extent than that of the hindcasts and twentieth century-RF simulations. Over North America and western Europe, the regions that show significantly enhanced skill over the twentieth century-RF simulations are larger than those of the hindcasts (Fig. 1a, d), indicating that considerably more skill may be achievable with better initialization techniques and improved models.

Skill in predicting North Atlantic SST on decadal timescales would imply, as described above, skill in initializing the Atlantic MOC. In the SST-restored simulations, the Atlantic MOC weakens from the

1950s till the mid-1960s, strengthens thereafter, peaking between the late-1980s to late-1990s, and subsequently weakens again (Fig. 2a). Although consistent with SST observations[25], the veracity of these results is hard to assess, as direct MOC observations are insufficient[8] and large uncertainties exist among ocean model simulations[21] and ocean analyses. The small ensemble spread relative to the low frequency MOC fluctuations also supports the utility of the initialization scheme.

In contrast to measurements of the MOC, regular hydrographic observations in the Labrador Sea extend back past the 1950s. As density changes in the Labrador Sea are widely accepted to force MOC variations[5,21,25], these observations provide an alternative method to assess MOC initialization. Simulated multidecadal fluctuations of wintertime Labrador Sea convection, weakest around 1970 and strongest in the early 1990s, broadly agree with observations of Labrador Sea Water thickness[26], which is closely related to convection (Fig. 2b). Furthermore, simulated MOC variations closely follow Labrador Sea convection by several years (Fig. 2). Thus, these results provide evidence that observed MOC fluctuations are, to a certain degree, skilfully initialized.

On multidecadal timescales, Labrador Sea convection is initialized directly by SST relaxation. The latter includes the history of observed atmospheric forcing, and in particular the North Atlantic Oscillation (NAO), which plays a key role in forcing multidecadal MOC variations[20,21,25]. Consistently, observed NAO variations lead simulated MOC changes by several years, but inconsistently, they are not well related to simulated Labrador Sea convection, except perhaps on multidecadal timescales (Fig. 2). Although the simulated NAO index does not correspond well with the observations, it strengthens during the simulated period, and thus probably also contributes to forcing MOC variations (Fig. 2c).

Initialized decadal fluctuations in the Atlantic MOC are predictable a decade in advance, with ensemble-spread small compared to the signal (Fig. 3a); hindcast skill is, however, largely due to capturing the long-term trend. MOC variations in the twentieth century-RF simulations are weak, and not surprisingly, unrelated to those in the initialization simulations. Model studies indicate that multidecadal Atlantic MOC variations force inter-hemispheric dipolar SST anomalies[5,7,14,16,19]. Observed variations of the latter are predicted a decade in advance by the hindcasts, but not by the twentieth century-RF simulations (Fig. 3b). Hindcast skill here is thus consistent with predicting Atlantic MOC variations. Consistently, North Atlantic (0–60° N) SST is better predicted by the hindcasts ($r = 0.77$) than the twentieth century-RF simulations ($r = 0.66$) (not shown). The
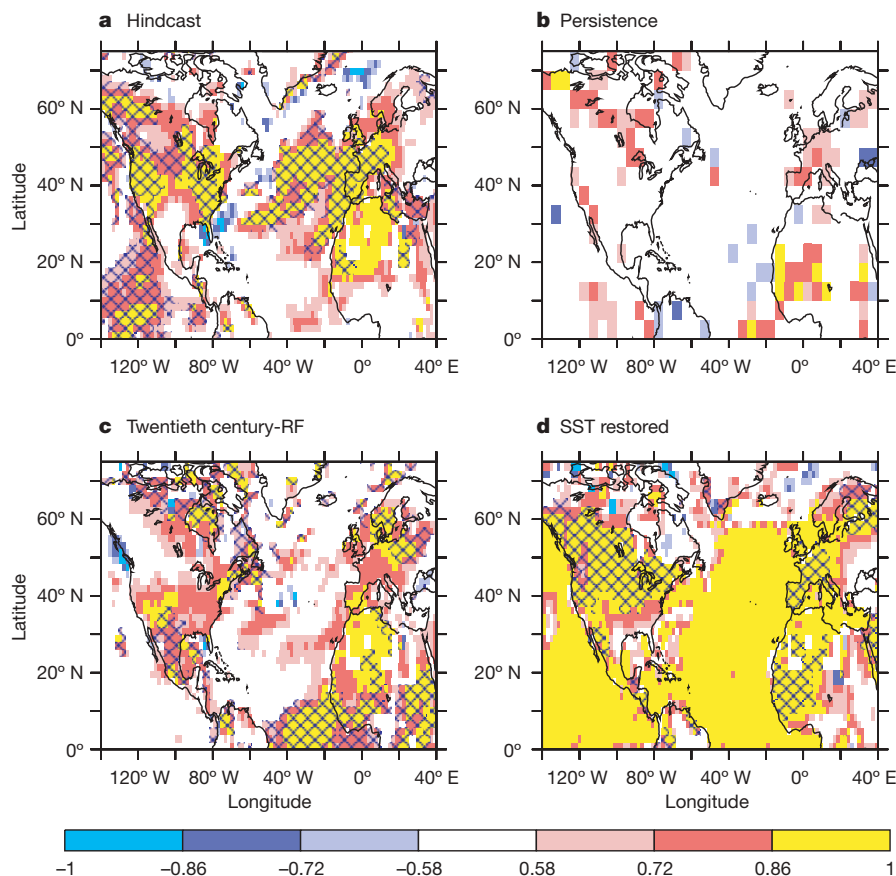

Figure 1 | Correlation skill in predicting observed ten-year mean surface temperature anomalies a decade in advance relative to other more traditional approaches. a, Skill of nine ten-year-long predictions, evenly distributed over the period 1955–2005, made with a climate model initialized using ocean (SST) observations and run with projected changes in radiative forcing. **b**, As in **a** but given by persistence. **c**, As in **a**, but not initialized using ocean observations and with radiative forcing following observations. **d**, As in **c**, but with model SST relaxed to observations between 60° S and 60° N (seen in near perfect correlations over the ocean). Correlations exceeding 0.58 are significant at the 5% level. Regions where initialization results in a significant enhancement or reduction in skill compared to radiative-forcing-only simulations are indicated by a blue cross-hatching in **a** and **c**, respectively. Land regions where restoring to observed SST anomalies provides a significant enhancement in skill relative to radiative-forcing-only simulations are indicated by blue cross-hatching in **d**. Correlations in **a** and **c** are field significant at close to the 0% level, while those in **b** pass the field significance test at the 1% level. Details of significance estimation are given in Methods. Correlations in **a**, **c** and **d** are computed from the ensemble mean of three simulations. SST observations are from HADISST[27]; land surface temperature observations are from CRUTEMP3[28].

greater skill of the hindcasts, over the twentieth century-RF simulations, in predicting decadal North Atlantic, western European (Figs 1 and 3c) and North American (Figs 1 and 3d) surface-temperature variations is thus likely to be due to skill in predicting Atlantic MOC fluctuations.

Enhanced skill over the twentieth century-RF simulations in predicting land surface temperature (Fig. 1a, c), especially over North America, may also arise from outside the Atlantic. In particular, tropical Pacific decadal SST variations are more skilfully predicted by the hindcasts, which correctly capture the 1970s climate shift, than by the twentieth century-RF simulations (Fig. 3e; Supplementary Information). Hindcast skill for global mean temperature (Fig. 4) is also high, but slightly less than the twentieth century-RF simulations. The largest difference occurs for the 1994–2004 predictions, with hindcast surface temperature cooler than observed and twentieth century-RF simulations warmer (Fig. 4). These differences stem from the predictions of internal tropical Pacific variability, with extreme warm conditions predicted by the twentieth century-RF simulations and near neutral conditions by the hindcasts;
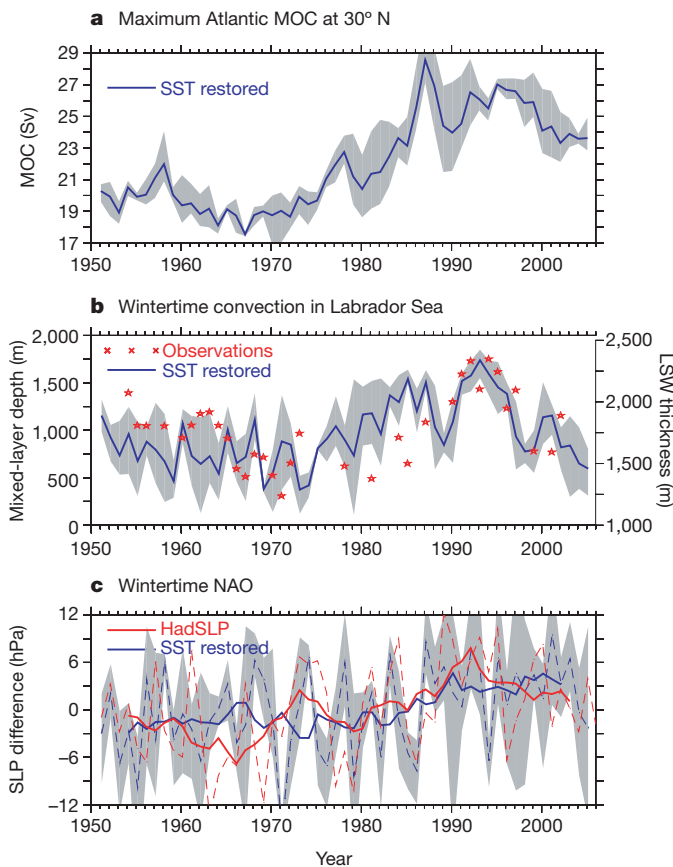

Figure 2 | SST restoring forces robust multidecadal fluctuations in the Atlantic Ocean meridional overturning circulation, Labrador Sea convection and the North Atlantic Oscillation. a, Annual mean meridional overturning circulation (MOC) at 30° N from the SST-restored simulations. Grey shading indicates ensemble spread in all panels. **b**, Simulated wintertime (December–February) Labrador Sea (60–50° W, 55–65° N) mixed-layer depth and observed annual mean Labrador Sea Water (LSW) thickness[26]. The latter is defined between isopycnals $\sigma_{1.5} = 34.72$–34.62, and is closely related to wintertime Labrador Sea convection. Simulated Labrador Sea convection precedes MOC variations at 30° N, with a maximum correlation (0.71) when the MOC lags by three years. **c**, Observed[29] and simulated ensemble mean wintertime North Atlantic Oscillation (NAO) indices. Solid lines indicate the seven-year running mean. The NAO index is defined as the sea-level-pressure (SLP) difference between Lisbon and Stykkisholmur. Observed NAO variations precede MOC variations at 30° N, with a maximum correlation (0.52) when the MOC lags by 3–4 years, but are not closely related to simulated Labrador Sea convection ($r < 0.4$ at any lag).
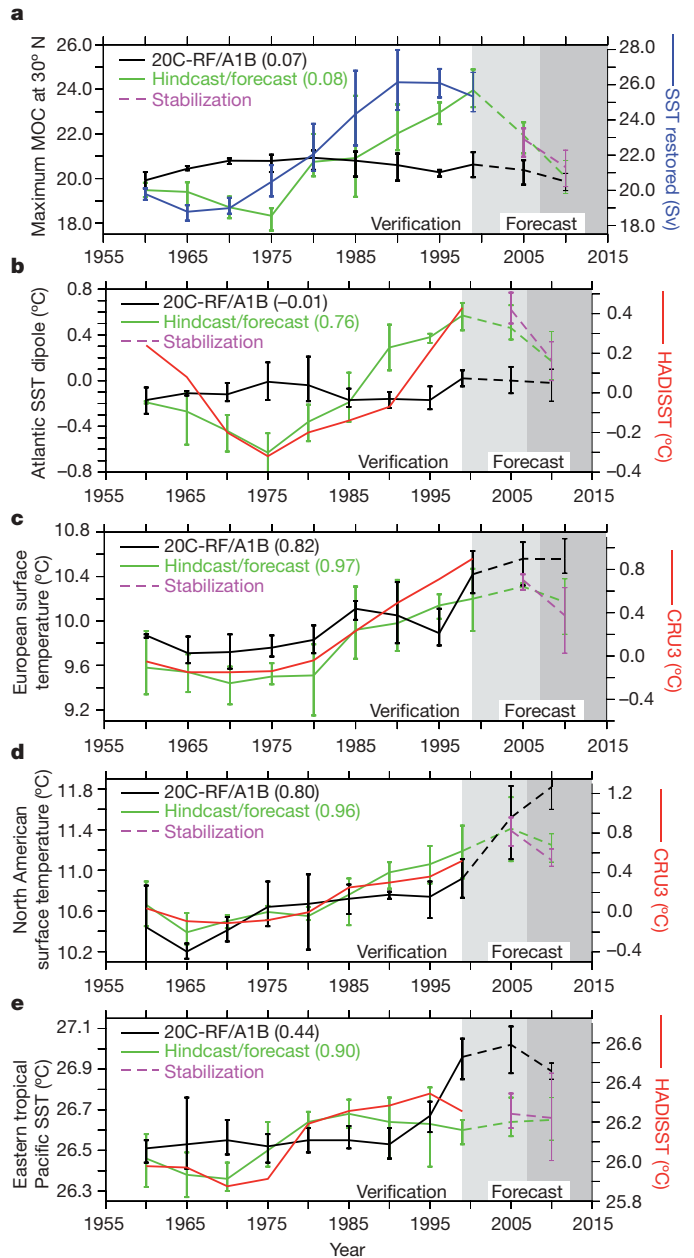

Figure 3 | Hindcast/forecast decadal means of selected time series, compared with observations and climate model projections including only radiative forcing changes but not initialized using ocean observations. Model projections are twentieth century-RF followed by A1B scenario simulations ('20C-RF/A1B'). **a**, Maximum MOC strength at 30° N; **b**, Atlantic SST dipole index (60–10° W, 40–60° N minus 50–0° W, 40–60° S SST area averages), which is constructed to isolate MOC forced SST fluctuations from radiatively forced variations[25]; **c**, European land surface temperature (5° W–10° E, 35–60° N average); **d**, North American surface temperature (120–70° W, 30–50° N average); and **e**, eastern Tropical Pacific SST (150–90° W, 20° S–20° N average). **a–e**, Each point represents a ten-year centred mean; vertical bars indicate ensemble spread; verification and forecast periods are indicated (dark shading begins 2008, indicating the start of the true forecast period); two additional forecasts with radiative forcing stabilized at year 2000 levels are also shown. **b–e**, Correlation of both hindcasts and climate model projections with observations are given in brackets. Owing to insufficient observations, in **a** the correlation with the MOC from SST-restored simulation is given. Hindcast correlation skill is significantly greater at the 5% level than that of the standard climate projection in all cases (significance test described in Methods). Scale on right is used for the SST-restored simulation and observations; note the different ranges for right and left axes in **a** and **b**. SST are from HADISST[27], land temperature from CRUTEMP3[28] ('CRU3').
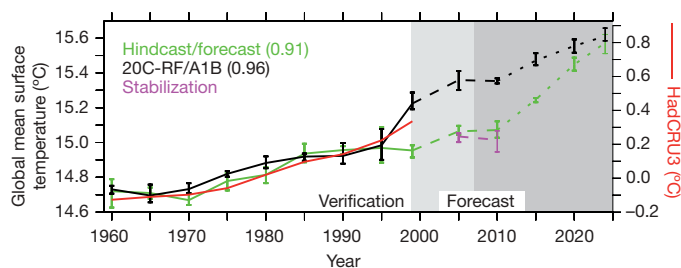
Figure 4 | Hindcast/forecast decadal variations in global mean temperature, as compared with observations and standard climate model projections. Model projections are twentieth century-RF followed by A1B scenario simulations ('20C-RF/A1B'); 'Stabilization' forecasts assume greenhouse gas concentrations fixed at year 2000 levels. Each point represents a ten-year centred mean; vertical bars indicate ensemble spread; verification and forecast periods are indicated (dark shading begins 2008, indicating the start of the true forecast period). Three additional decadal means (joined by a dotted line) show the evolution of the initialized and un-initialized 2005 predictions extended till 2030. Correlation of both hindcasts and climate model projections with observations are given in brackets. Correlation of the twentieth century-RF simulation with observations is greater than that of the hindcasts, but only marginally at the 5% significance level. Observed global mean temperature anomalies are from HadCRU3[28].

weak warm conditions were observed (Fig. 3e; Supplementary Information).

We now consider two forecasts, started in November 2000 and November 2005. The MOC is predicted to weaken almost to its 1950–2005 mean over the next decade (Fig. 3a), leading to a weakening of Atlantic SST hemispheric difference towards zero (Fig. 3b). North Atlantic (not shown), western European (Fig. 3c) and North American (Fig. 3d) surface temperatures cool towards 1994–2004 levels. In contrast, in the un-initialized (twentieth century-RF) predictions the MOC slightly weakens, the hemispheric SST difference is unchanged, and warming of surface temperatures over the latter three regions continues (Fig. 3a–d). Eastern tropical Pacific SST is forecasted to remain almost unchanged, but 0.3 K cooler than the un-initialized predictions (Fig. 3e). The differences in predicted North Atlantic and tropical Pacific variability lead to a large difference in the global mean temperature prediction: the initialized prediction indicates a slight cooling relative to 1994–2004 levels, while the anthropogenic-forcing-only simulation suggests a near 0.3 K rise (Fig. 4). In the long-term both projections agree with each other, as is found by extending the 2005 prediction till 2030 (Fig. 4). Internal decadal fluctuations were also found to offset anthropogenic global warming in a previous study[19], but the offset was much less pronounced and associated primarily with changes in the tropical Pacific.

To investigate the sensitivity of the predictions to greenhouse gas forcing only, the two forecasts were repeated assuming that greenhouse gases were stabilized at year 2000 values. The predictions for the MOC and surface temperature remain basically unchanged. Thus, in the near future, natural decadal variability in the Atlantic and Pacific may not only override the regional effects of global warming, but temporarily weaken it. Thus, a joint initial/boundary value problem has to be considered when forecasting North Atlantic sector and global climate variability for the coming decades.

The results presented here are promising in light of existing model biases. Experience in numerical weather prediction and seasonal forecasting has shown that skill can be considerably improved by reducing model systematic error and by more accurate forecast initialization. Thus, useful decadal predictions may be in reach.

METHODS SUMMARY

Simulations. Results are based on three sets of simulations with the ECHAM5/MPI-OM coupled general circulation model[24] (IPCC version). (1) Three integrations (twentieth century-RF/A1B), from 1860–2015, started from different points of a control simulation. Before 2000, radiative forcing follows

observations (greenhouse gas and sulphate aerosol concentrations, solar cycle variations, and major volcanic eruptions), and after 2000, it follows the IPCC A1B scenario. Predictability due to radiative forcing is estimated from these simulations. (2) Three coupled integrations (SST-restored), from 1950–2005, initialized from the twentieth century-RF simulations and with identical radiative forcing, but with relaxation towards SST constructed from the coupled model climatology with observed SST anomalies superimposed. The relaxation constant is strong ($0.25\,d^{-1}$) between 30° S and 30° N, and decreases linearly to zero between 30° and 60° S and between 30° and 60° N; poleward of 60° S and 60° N the model is fully coupled. (3) Nine hindcasts and two forecasts (three-member, ten-years long), initialized from the SST-restored simulations during the period 1955–2005. Radiative forcing is as in the twentieth century-RF simulations, except for solar cycle variations, which are repeated from the previous 11 years, and major volcanic eruptions. The latter that occurred during a hindcast are not included, and the impact of any that occurred before the hindcast is damped away with an e-folding time of one year.

Significance tests. For nine forecasts we assume seven degrees of freedom (d.f.). As only positive correlations indicate skill, the significance level for the forecast is determined using a one-sided t-test. A correlation is determined to be significantly larger or smaller than another if the Fisher-Z transformed values pass a one-sided t-test for differences in means (with 12 d.f.). The Fisher-Z distribution of correlations of nine independent and normally distributed pairs of points is close to normal. Field significance is estimated on a 15° × 15° grid to minimize effects of spatial correlation.

1. Goldenberg, S. B., Landsea, C. W., Mestas-Nuñez, A. M. & Gray, W. M. The recent increase in Atlantic hurricane activity: Causes and implications. *Science* **293**, 474–479 (2001).
2. Enfield, D. B., Mestas-Nuñez, A. M. & Trimble, P. J. The Atlantic Multidecadal Oscillation and its relation to rainfall and river flows in the continental U. S. *Geophys. Res. Lett.* **28**, 2077–2080 (2001).
3. Sutton, R. T. & Hodson, D. L. R. Atlantic Ocean forcing of North American and European summer climate. *Science* **309**, 115–118 (2005).
4. Folland, C. K., Palmer, T. N. & Parker, D. E. Sahel rainfall and worldwide sea temperatures, 1901–85. *Nature* **320**, 602–607 (1986).
5. Griffies, S. M. & Bryan, K. Predictability of North Atlantic multidecadal climate variability. *Science* **275**, 181–184 (1997).
6. Boer, G. A study of atmosphere-ocean predictability on long time scales. *Clim. Dyn.* **16**, 469–472 (2000).
7. Collins, M. *et al.* Interannual to decadal climate predictability in the North Atlantic: A multimodel-ensemble study. *J. Clim.* **19**, 1195–1203 (2006).
8. Cunningham, S. A. *et al.* Temporal variability of the Atlantic meridional overturning circulation at 26.5°N. *Science* **317**, 935–938 (2007).
9. Smith, D. M. *et al.* Improved surface temperature prediction for the coming decade from a global climate model. *Science* **317**, 796–799 (2007).
10. Solomon, S. *et al. Climate Change 2007: The Physical Science Basis* (Cambridge Univ. Press, Cambridge, UK, 2007).
11. Bjerknes, J. Atlantic air-sea interaction. *Adv. Geophys.* **10**, 1–82 (1964).
12. Kushnir, Y. Interdecadal variations in North Atlantic sea surface temperature and associated atmospheric conditions. *J. Clim.* **7**, 141–157 (1994).
13. Schlesinger, M. E. & Ramankutty, N. An oscillation in the global climate system of period 65–70 years. *Nature* **367**, 723–726 (1994).
14. Knight, J. R., Allan, R. J., Folland, C. K., Vellinga, M. & Mann, M. E. A signature of persistent natural thermohaline circulation cycles in observed climate. *Geophys. Res. Lett.* **32**, doi:10.1029/2005GL024233 (2005).
15. Mann, M. E., Bradley, R. S. & Hughes, M. K. Global-scale temperature patterns and climate forcing over the past six centuries. *Nature* **392**, 779–787 (1998).
16. Delworth, T., Manabe, S. & Stouffer, R. J. Interdecadal variations of the thermohaline circulation in a coupled ocean-atmosphere model. *J. Clim.* **6**, 1993–2011 (1993).
17. Vellinga, M. & Wu, P. Low-latitude freshwater influence on centennial variability of the Atlantic thermohaline circulation. *J. Clim.* **17**, 4498–4511 (2004).
18. Jungclaus, J. H., Haak, H., Latif, M. & Mikolajewicz, U. Arctic North Atlantic interactions and multidecadal variability of the meridional overturning circulation. *J. Clim.* **18**, 4013–4031 (2005).
19. Latif, M., Collins, M., Pohlmann, H. & Keenlyside, N. A review of predictability studies of the Atlantic sector climate on decadal time scales. *J. Clim.* **19**, 5971–5987 (2006).
20. Eden, C. & Jung, T. North Atlantic interdecadal variability: Oceanic response to the North Atlantic oscillation (1865–1997). *J. Clim.* **14**, 676–691 (2001).
21. de Coëtlogon, G. *et al.* Gulf Stream variability in five oceanic general circulation models. *J. Phys. Oceanogr.* **36**, 2119–2135 (2006).
22. Keenlyside, N., Latif, M., Botzet, M., Jungclaus, J. & Schulzweida, U. A coupled method for initializing El Niño Southern Oscillation forecasts using sea surface temperature. *Tellus A* **57**, 340–356 (2005).
23. Lee, T. C. K., Zwiers, F., Zhang, X. & Tsao, M. Evidence of decadal climate prediction skill resulting from changes in anthropogenic forcing. *J. Clim.* **19**, 5305–5318 (2006).

24. Jungclaus, J. H. *et al.* Ocean circulation and tropical variability in the coupled model ECHAM5/MPI-OM. *J. Clim.* **19**, 3952–3972 (2006).
25. Latif, M. *et al.* Is the thermohaline circulation changing? *J. Clim.* **19**, 4631–4637 (2006).
26. Curry, R. G., McCartney, M. S. & Joyce, T. M. Oceanic transport of subpolar climate signals to mid-depth subtropical waters. *Nature* **391**, 575–577 (1998).
27. Rayner, N. A. *et al.* Global analyses of sea surface temperature, sea ice, and night marine air temperature since the late nineteenth century. *J. Geophys. Res.* **108**, 4407, doi:10.1029/2002JD002670 (2003).
28. Brohan, P., Kennedy, J. J., Harris, I., Tett, S. F. B. & Jones, P. D. Uncertainty estimates in regional and global observed temperature changes: a new dataset from 1850. *J. Geophys. Res.* **111**, D12106, doi:10.1029/2005JD006548 (2006).
29. Allan, R. & Ansell, T. A new globally-complete monthly historical gridded mean sea level pressure data set (HadSLP2): 1850–2004. *J. Clim.* **19**, 5816–5842 (2006).